



Effect of phospholipid-protein interfacial interactions on the aeration emulsion quality during reconstitution of fat globule membranes: Interfacial behavior, thermodynamic properties, stability and whipping properties

Guosen Yan^{a,b,1}, Pan Zhao^{a,1}, Zhenbo Shao^b, Yiting Li^b, Jie Han^b, Yan Li^{a,*}, Liebing Zhang^b

^a Beijing Engineering and Technology Research Centre of Food Additives, School of Food and Health, Beijing Technology and Business University, Beijing 100048, China

^b College of Food Science and Nutritional Engineering, China Agricultural University, Beijing 100083, China

ARTICLE INFO

Keywords:

Phospholipid
Interface behavior
Crystallization kinetics
Aerated emulsion

ABSTRACT

This study examines the interaction between phospholipids (PL) and proteins during the reconstitution of milk fat globule membranes (MFGM) and their effects on structure, properties, and fat crystallization behavior. Adding 0–0.45 % PL altered the MFGM composition, reduced interfacial protein concentration ($27.49\text{--}37.88 \times 10^{-4} \text{ g/m}^2$), interfacial tension ($11.05\text{--}15.23 \text{ mN/m}$), and droplet sizes ($1.53\text{--}2.16 \mu\text{m}$), while increasing viscosity ($20.39\text{--}25.11 \text{ mPa s}$), thus enhancing emulsion stability. High PL concentrations caused skin-like folding, increasing interfacial protein content ($29.23\text{--}29.52 \times 10^{-4} \text{ g/m}^2$) and droplet aggregation ($1.68\text{--}1.71 \mu\text{m}$). PL acted as a non-homogeneous nucleating agent, increasing microcrystal formation and nucleation sites but reducing initial crystallization temperature. The reduced mechanical strength of the MFGM decreased cream churning time and overrun, while higher viscosity reduced serum loss and increased hardness. These findings provide insights for improving aerated emulsion quality.

1. Introduction

Cream is a popular traditional dairy product that is widely used in baking and cake and dessert decoration. Industrial manufacturers are meeting the growing global demand for recombined dairy cream (RDC) by standardizing the production of anhydrous milk fats (AMF), water, and emulsifiers. From a microscopic perspective, RDC can be described as a typical oil-water (O–W) aeration emulsion, where droplets are dispersed in a continuous phase to stabilize the RDC emulsion. In addition, a high-quality RDC must also display good whipping characteristics.

The fat globules in cow's milk are covered by membranes consisting of three layers of PL and functional proteins, providing the spatial and physical barriers needed for stability (Thum et al., 2023). The AMF used in RDC destroys the natural fat globule membrane and separates the internal milk fat for commercial production. This process is reversed during RDC production. The bulk milk fat is dispersed under turbulence/shear into fat microspheres during a continuous aqueous RDC emulsion

phase, causing stable fat globule reformation and fat globule membrane remodeling. MFGM are formed by the adsorption and rearrangement of small molecules such as proteins and emulsifiers during the continuous phase under shear. Therefore, the MFGM structure and properties are determined, to some extent, by the selection and use of emulsifiers, which may further affect the RDC quality.

PL is the main component of natural fat globule membranes, consisting of a hydrophilic head (polar part) and two hydrophobic aliphatic chains (non-polar part). The head contains a phosphate group (negatively charged) bonded to choline (quaternary ammonium salt, positively charged) via an ester bond to form a dyadic ionic structure. The hydrophobic fatty acid chains of PL are embedded in the oil droplets at the O–W interface. The hydrophilic head reaches out to the aqueous phase, lowering the interfacial tension and forming a complete interfacial film that encapsulates the droplets to stabilize the emulsion (Gutiérrez Méndez et al., 2022). This facilitates excellent emulsification, allowing extensive application in food products such as meat, sauces, puddings, and fillings. Bernaschina et al. (2024) used PL to prepare lentil

* Corresponding author.

E-mail address: liyan@btbu.edu.cn (Y. Li).

¹ Guosen Yan and Pan Zhao contributed equally to this study.

protein emulsions, showing that the addition of 0.25 % PL reduced droplet size and emulsion aggregation. Another study confirmed the positive impact of PL on low-fat RDC stability (Zhou et al., 2016). In addition, competitive PL and protein adsorption altered the MFGM composition. Lu et al. (2021) revealed that PL addition before milk homogenization altered the surface structure and composition of the MFGM, while protecting the original milk proteins to some extent. PL reportedly facilitates a four-fold higher interfacial protein load than sodium caseinate alone, which increased the interfacial layer thickness (Yesiltas et al., 2019). In addition, the presence of PL alters the hydrodynamic thickness of the adsorbed protein layer on hydrophobic oil surfaces. Current research indicates that protein-phospholipid complexes can influence the stability of emulsions, though their interfacial behavioral mechanisms remain poorly characterized. While existing research predominantly focuses on functional characterization of RDC, systematic elucidation of phospholipid-protein synergies during fat globule membrane reorganization is notably absent. The implications of these mechanistic gaps on RDC systems urgently warrant further investigation.

Crystallization-mediated partial aggregation is thought to be crucial for churning inflation in the RDC system, while fat globules are bound and stabilized by crystal bridging to form a network structure for gas bubble binding and stabilization (Goibier et al., 2019). Emulsifiers act as nucleation sites on MFGMs to alter the crystallization behavior of fat, such as promoting or inhibiting fat nucleation, crystal growth, polycrystalline transformation, and crystal interactions. Furthermore, PL may influence the crystallization properties of the lipid system (Patel & Dewettinck, 2015). Svanberg et al. (2011) revealed that the presence of PL significantly affected the crystallization kinetics of chocolate, by acting as nucleation sites for fat crystallization. Atik et al. (2020) indicated higher PL content and lower polyglycerol polyricinoleate levels caused β polycrystal formation in milk chocolate. Contrarily, Cooper et al. (2019) showed that higher PL concentrations reduced AMF crystallization and caused crystal morphology variation. However, no studies are available regarding the effect of PL on the RDC aeration properties.

This study examines the role of PL in MFGMs and the mechanisms that influence RDC stability and whipping properties. RDC samples are prepared using different PL concentrations for stability. The effect of PL on the RDC droplet size, microstructure, stability, rheological properties, whipping properties, interfacial loading, surface tension, and strength are also analyzed. The changes in the thermodynamic properties of the fat and crystalline morphology due to PL are assessed to evaluate the potential of PL application in the RDC system.

2. Materials and methods

2.1. Materials

The AMF was obtained from Anchor, New Zealand, the main fatty acids include short-chain saturated fatty acids (3 %), medium-chain saturated fatty acids (10 %), long-chain saturated fatty acids (48 %), and unsaturated fatty acids (37 %) (Li et al., 2024). While Ningxia Saishang Dairy, China, provided the milk protein concentrate (MPC, 70 % protein). The PL was acquired from Cargill Asia-Pacific, China, and its primary component is soybean lecithin. While FMC, USA, supplied the microcrystalline cellulose, and Merck, China, provided the Florisil (60–100 mesh). The Nile Red (NR) and fluorescein isothiocyanate (FITC) was obtained from Solarbio, China. All other reagents were analytically pure.

2.2. Preparation of RDC

RDC is formulated with deionized water, AMF (36 %), MCC (0.03 %), protein (1.60 %), and emulsifiers (0.0–0.75 %). PL, MCC, and proteins were added to deionized water, thoroughly dissolved, and then

uniformly mixed with melted AMF. The two solutions were subsequently mixed using an overhead mechanical stirrer at 70 °C (700 rpm, 30 min). Next, the emulsion is homogenized using a two-stage homogenizer at 4 + 2 MPa, after which the RDCs are stored at 4 °C for 24 h. The RDC preparation process was repeated at least three times.

2.3. Average droplet size and size distribution

The particle sizes of the samples were determined via wet measurement using a particle size analyzer (Mastersizer 3000, Malvern). The samples were added dropwise to a cuvette until reaching an opacity between 10 and 20 %. A Hydro LV detector was employed for determination using water as a dispersant, a stirring speed of 2500 rpm, and a refractive index of 1.33. The measurement was repeated three times. $D_{[3,2]}$ was used to represent the particle sizes of the samples:

$$D_{[3,2]} = \frac{\sum n_i d_i^3}{\sum n_i d_i^2} = \frac{\sum d^3}{\sum d^2} \quad (1)$$

where d_i represents the droplet diameter, and n_i denotes the number of droplets with d_i diameters in the RDC emulsion.

2.4. Confocal laser scanning microscopy

The microstructures of the samples were observed using confocal laser scanning microscopy (CLSM). Here, 1 mL of RDC emulsion was diluted five-fold with ultrapure water, after which 20 μ L of NR (0.02 %) and FITC (0.02 %) were added separately while avoiding light. The CLSM parameters included an argon lamp as the excitation light source, an excitation light wavelength of 488 nm (20 mV) for both NR and FITC, and reception wavelengths of 595–648 nm and 500–536 nm, respectively (Xu et al., 2024).

2.5. Physical stability

The stability of the RDC was determined using a LUMiSizer full-featured stability analyzer (LUM, Germany). The instability index was obtained during the accelerated centrifugal gravitational settling process by recording the transmittance of NIR light at different positions in the cuvette over time. A smaller index indicated that the sample was fairly stable. The test parameters included a temperature of 25 °C, a rotational speed of 1878.24 g, and a time interval of 30 s, while 90 measurements were performed.

2.6. Steady shear flow

A Physical MCR 301 rheometer (Anton Paar, Austrian) was employed to determine the steady shear flow of the RDC samples within 24 h of preparation at a test temperature of 25 °C, while the shear rate was increased evenly from 0 to 200 s^{-1} over 420 s. All samples were equilibrated for 5 min before testing. The samples were measured three times in parallel (Wang et al., 2019).

2.7. Apparent viscosity

The apparent viscosity of the samples was determined using a previously delineated method with slight modifications (Yan, Wang, et al., 2022). The apparent viscosity was measured for 60 s at 3 s intervals using a Brookfield DV3T viscometer equipped with an SC4–18 rotor at a speed of 30 rpm.

2.8. Interfacial protein concentration

The interfacial protein load was determined using a previously described. Here, 15 g of the sample was placed in a 50 mL tube and centrifuged for 1 h at 4 °C and a centrifugal force of 10,000 g, after which

the lower layer of clear liquid and precipitate were removed. The protein content in the clear liquid was determined via the Kjeldahl method, while the interfacial protein loading Γ was calculated as follows:

$$\Gamma (\text{mg}/\text{m}^2) = \frac{m - m_1}{F_m \times \text{SSA}} \quad (2)$$

where m represents the total protein amount (mg), m_1 denotes the liquid phase protein amount (mg), F_m is the mass of the dispersed phase (mg), and SSA represents the specific surface area (m^2/g), as determined in Section 2.3.

2.9. Z-potential

The emulsion samples were diluted 500-fold in deionized water, after which their potential was determined using a Nano90 analyzer (Malvern, UK). The diluted samples were slowly added to the potentiometric cuvette (DTS1070) to avoid air bubbles. The measurement parameters included an assay temperature of 25 °C, an absorbance of 0.001, and an equilibration time of 3 min. Each sample was measured three times.

2.10. Interfacial behavior

The pendant drop method was employed to assess the adsorption kinetics and oscillatory dilatational rheology of different PL and protein concentrations at the O–W interface. An interfacial tensiometer (Theta Flex Biolin Scientific AB, Sweden) was employed to document the morphology of the suspended droplets using a high-speed video camera. The time-tension curves were obtained via the Young-Laplace equation using the ADVANCE software. The AMF was purified with Florisil and placed in a cuvette. Then, protein solutions containing various PL concentrations were injected into the oil phase to obtain a 15 μL suspension. The surface tension (σ , mN/m) as a function of time was measured at 42 °C for 3600 s (Yan et al., 2024).

Next, the oscillatory dilatational rheology of the interfacial layer was analyzed. Periodic interfacial compression and expansion were achieved by increasing and decreasing the droplet volume at an amplitude of 0.7 μL and a frequency of 0.1 Hz. The recorded data were analyzed using ADVANCE to obtain the dilatational elastic modulus (E') and viscous modulus (E'') of the surfaces.

2.11. Differential scanning calorimetry

The thermal behavior of the RDC was analyzed via differential scanning calorimetry (DSC-Q200, TA, USA). A 10 mg sample was sealed in an aluminum box, while an empty aluminum box was used as a control. Nitrogen was used to purify the system. The DSC sample disk was maintained at 45 °C for 2 min to eliminate historical crystallization. Then, the RDC crystallization profile was obtained by lowering the temperature to –20 °C at a rate of 5 °C/min, where it was maintained at –20 °C for 2 min. Next, the temperature was increased to 45 °C at a rate of 5 °C/min to acquire the RDC melting curve (Wang et al., 2019).

2.12. Crystallization kinetics

The DSC data were used to analyze the non-isothermal kinetics of the RDC emulsions containing different PL concentrations (Cheng et al., 2021). The Avrami model was employed to determine the fat crystallinity variation over time (Eq. 3):

$$X(t) = 1 - \exp(-kt^n) \quad (3)$$

where $X(t)$ is the relative crystallinity at time t , n is the Avrami exponent and relates to the crystal growth geometry, and k is the crystallization rate constant.

For calculation convenience, Eq. (3) can be re-written as follows:

$$\lg(-\ln(1-X(t))) = \lg k + n \lg t \quad (4)$$

When $\lg(-\ln(1-X(t)))$ is plotted versus $\lg t$, the intercept is $\lg k$, and the slope is n .

2.13. Fat crystal microstructure

The microstructures of the fat crystals in the RDC emulsion were observed via polarized light microscopy (PLM). The RDC emulsions were stirred for 1 min at 10,000 rpm using a high-speed stirrer (IKA T25, Staufen, Germany) instead of a high-pressure homogenizer. A 10 μL drop of the RDC emulsion was placed on a slide and allowed to crystallize at 4 °C for 24 h before observation.

2.14. Whipping properties

After storage for 24 h, a 200 g sample was placed in a container and whisked using a mixer (AHM-P125A, North American). The endpoint of the churn was determined by the ability to create an upright cone with no visible fat particles (Wang et al., 2019), and the whipping time was recorded immediately. The overrun of the whipped cream was determined by the change in mass of the same volume before and after whipping and was calculated as follows:

$$\text{overrun} (\%) = \frac{m_1 - m_2}{m_2} \times 100\% \quad (5)$$

where m_1 and m_2 represent the mass of the RDC before and after whipping, respectively.

2.15. Serum loss

A certain quantity of whipped cream was placed in a 30-mesh sieve with a diameter of 5 cm and inserted into a constant temperature incubator at 30 °C for 2 h to determine the degree of serum loss. The serum loss is calculated as follows:

$$\text{serum loss} (\%) = \frac{m_2}{m_1} \times 100 \quad (6)$$

where m_1 and m_2 represent the amount of cream at the end of the churning process and the degree of loss (Zeng et al., 2022).

2.16. Textural analysis

A texture meter equipped with an HDP/FE3 probe (TA-XT2i, TA, USA) was used to analyze the whipped cream texture at a trigger force of 0.5 N, a determination speed of 1 mm/s, and a penetration depth of 30 mm. Each sample was tested at least three times.

2.17. Statistical analysis

All experiments were repeated at least three times to avoid errors, and the results were expressed as mean \pm SD. One-way analysis of variance (ANOVA) was performed using SPSS 20.0. Differences were considered statistically significant when $p < 0.05$.

3. Results and discussion

3.1. Characterization of the RDC emulsions

3.1.1. Average droplet size and size distribution

Fat globule size is crucial for the stability of cream during processing and storage (Dhungana et al., 2019), while the nature and concentration of the emulsifier vitally affect the emulsion droplet size (Koocheki et al., 2009). Fig. 1A shows the droplet size distribution in the RDC emulsion before adding the different PL concentrations. The droplet size of the

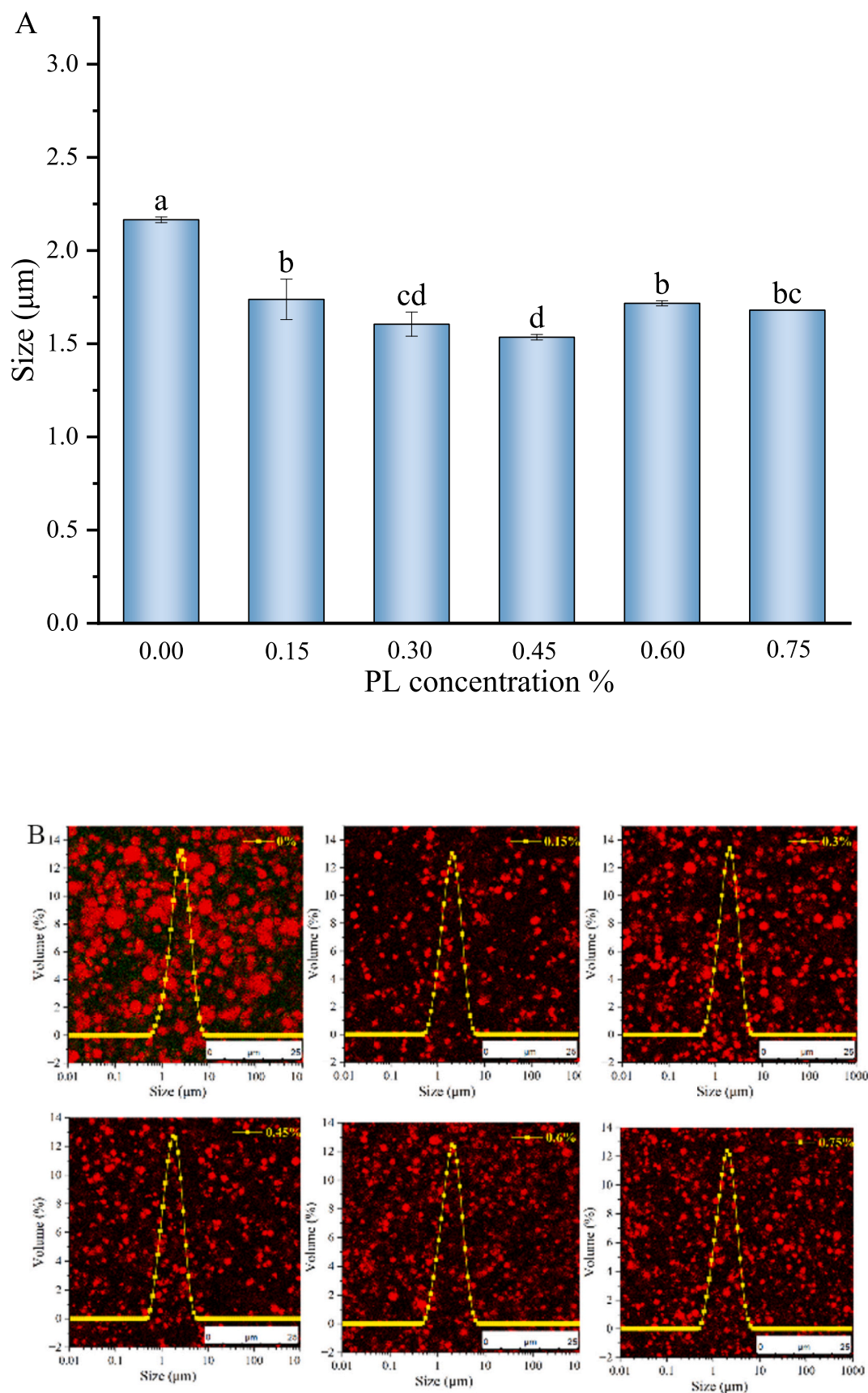


Fig. 1. Effect of different PL concentrations on droplet size (A) and size distribution (B) of RDC emulsions. Different letters indicate statistically significant differences between samples ($p < 0.05$).

control group without added PL was about 2.17 μm , which was significantly higher than in the samples containing PL. This indicated PL significantly reduced the fat globule size, regardless of the concentration. In a range of 0–0.45 %, the droplet size decreased gradually as the PL concentration increased, exhibiting the smallest particles of 1.54 μm at 0.45 % ($p < 0.05$). Fig. 1B shows the distribution of the different droplets, with only one particle size distribution peak for all samples, indicating that the addition of PL resulted in a more uniform distribution of the fat globule sizes and a clearer peak shape. The fat globule particle size increased as the concentration continued to rise (>0.45 %). This suggests that high PL concentrations are detrimental to droplet dispersion.

3.1.2. Physical stability of the RDC emulsions

The physical stability of the samples was evaluated by monitoring the phase separation during gravitational acceleration via near-infrared light. Fig. 2 shows the instability index of the samples. The results indicated that the control group without PL displayed the highest instability index (0.21), which declined to 0.08 when the PL concentration was increased from 0.00 % to 0.15 %, with a significant rise in physical stability ($p < 0.05$). The instability index of the RDC emulsion decreased further at a higher PL concentration, displaying the lowest value of 0.04 at 0.75 %. This suggests that PL addition contributes to the physical stability of the emulsion and is positively correlated with the concentration. Notably, the instability index was not statistically different ($p > 0.05$) at concentrations higher than 0.3 %, indicating that O–W interface formation was no longer limited by the PL concentration.

3.1.3. Rheological properties of the RDC emulsions

The rheological behavior of the RDC containing different PL

concentrations was analyzed via steady shear rheology. As shown in Fig. 3A, all the PL reconstituted RDC samples were pseudoplastic liquids. A higher shear rate dramatically decreased the viscosity within 30 s, followed by stabilization, which was related to the destruction of flocs inside the RDC emulsion during shear (Liu et al., 2022). In addition, a higher PL concentration increased the viscosity and shear pressure of the RDC emulsion during the shear process. Fig. 3B shows the shear viscosity at 30 rpm. PL concentrations of 0.6 % and 0.75 % significantly increased the RDC emulsion viscosity to 28.55 mPa \bullet s and 30.74 mPa \bullet s, respectively. This may be because PL addition changes the droplet size, increasing the mutual collision during flow (Pal, 1998). The viscosity of the 0.75 % PL RDC emulsion increased rapidly at high shear rates. Fredrick et al. (2013) explored the viscosity profile of natural cream at a constant shear rate, revealing a sudden increase in sample viscosity after a long lag phase. Analysis of the sample microstructures indicated that the increased viscosity could be attributed to the formation of large fat coalescences and reticulations. This was consistent with the findings of Ihara et al., 2015 regarding natural cream and RDC samples. These results suggest that PL addition may affect the MFGM strength and the fat globule stability, which are prone to rupture and coalescence during flow.

3.2. Interfacial protein content

The protein content of fat globule membranes was analyzed to further investigate the effect of PL on MFGM. During RDC emulsion formation, protein adsorption at the O–W interface and stable viscoelastic protein layer formation are closely related to the physical strength of the fat globule membrane (Yan et al., 2024). Fig. 4 shows the interfacial protein concentrations of the different samples. The results showed that the blank fraction displayed the highest interfacial protein

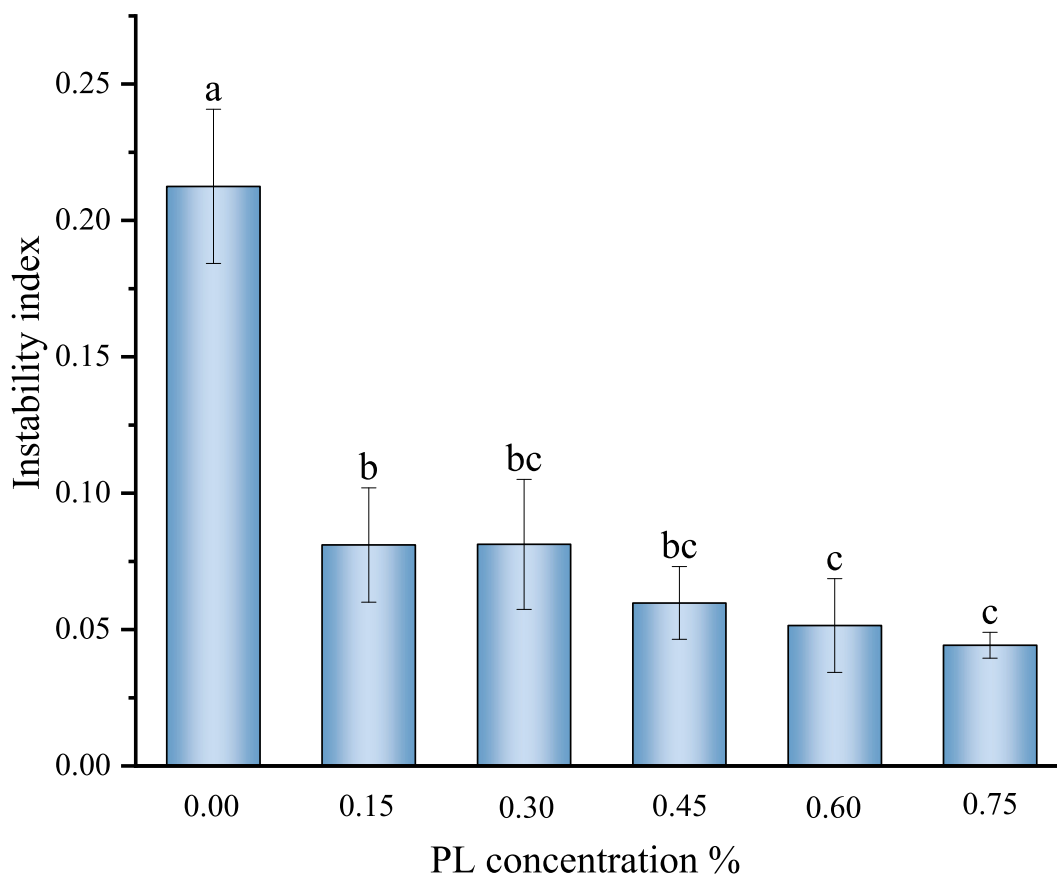


Fig. 2. Effect of different PL concentrations on the instability index of RDC emulsions. Different letters indicate statistically significant differences between samples ($p < 0.05$).

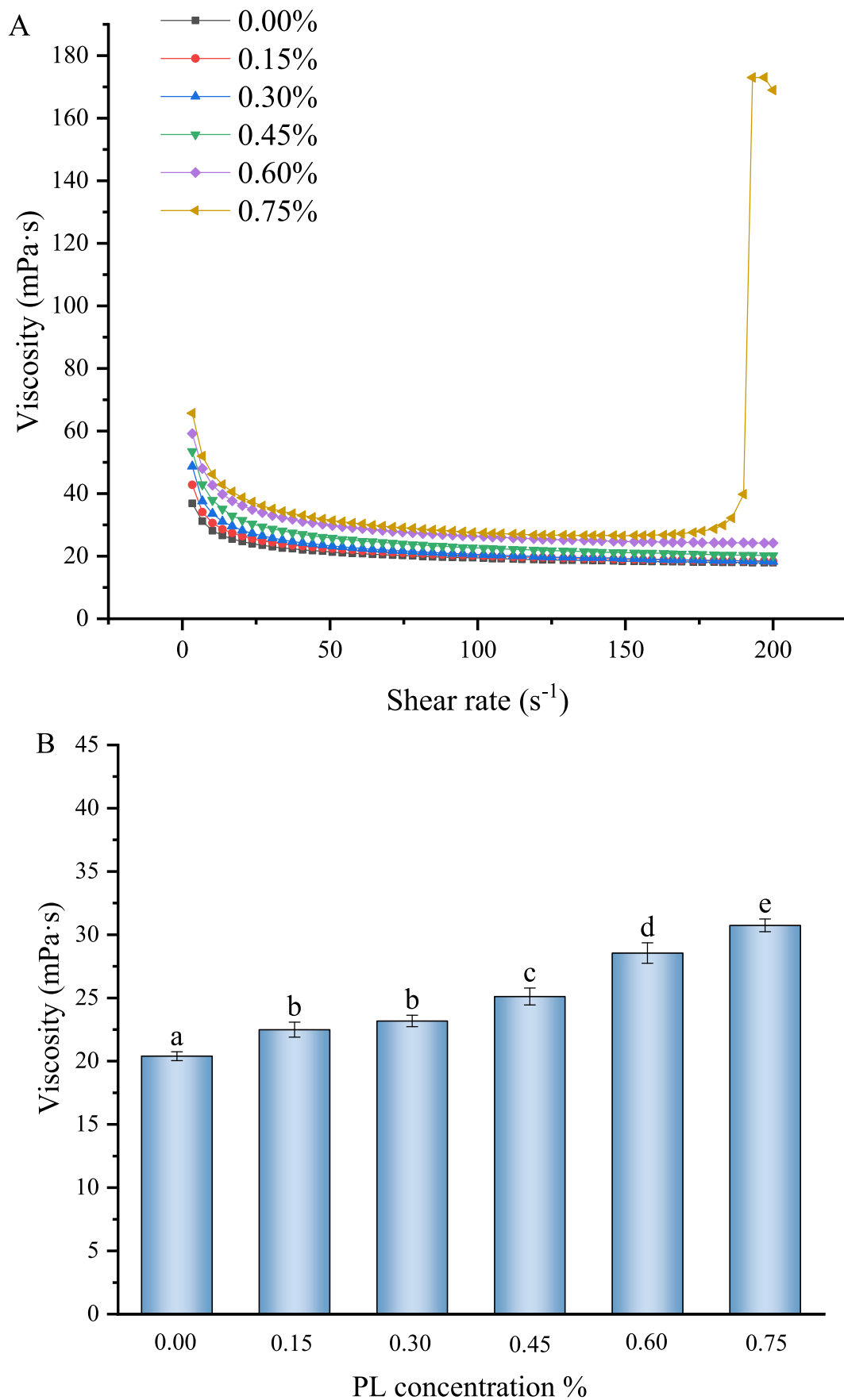


Fig. 3. Effect of different PL concentrations on the steady shear rheology of emulsions. (A) and viscosity (B). Different letters indicate statistically significant differences between samples ($p < 0.05$).

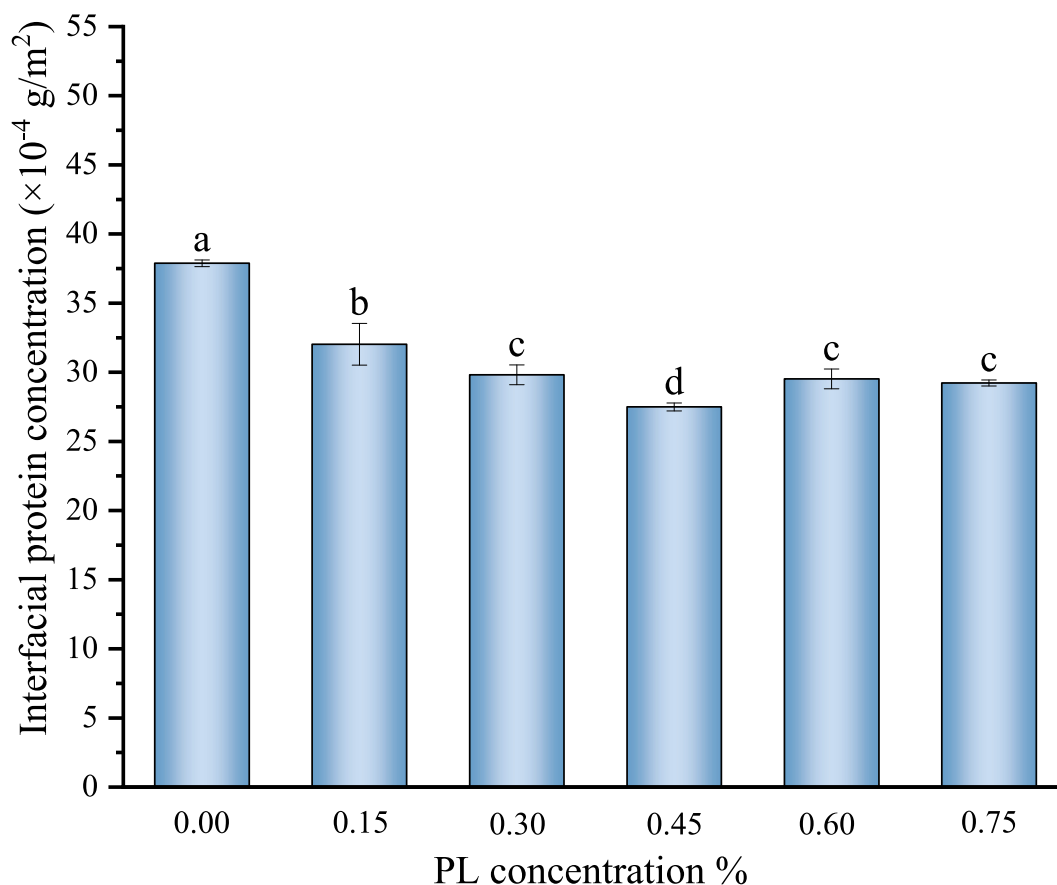


Fig. 4. Effect of different PL concentrations on the interfacial protein concentration of RDC emulsions. Different letters indicate statistically significant differences between samples ($p < 0.05$).

content at 37.88×10^{-4} g/m². PL addition significantly decreased the interfacial protein concentration ($p < 0.05$), which showed the lowest value of 27.49×10^{-4} g/m² at a 0.45 % PL concentration. Contrarily, higher PL concentrations (>0.45 %) substantially increased the interfacial protein levels. The fat globule surfaces in the control group were completely stabilized by milk protein layer formation. Although the thicker protein layer at the interface prevented coalescence due to fat crystallization (Cheng et al., 2020), the proteins displayed a limited ability to reduce the tension, consequently forming larger droplets (2.17 μ m). Studies have shown that emulsifiers compete with proteins for adsorption at the O–W interface. The PL had a lower molecular weight than the proteins, allowing more rapid adsorption to the O–W interface during interfacial formation (Yan, Yang, et al., 2022). When gaps were present between the adsorbed proteins at the O–W interface, the exposed droplet surface provided a hydrophobic region for PL adsorption. A higher adsorbed PL concentration compressed the interfacial proteins, leading to bulging and even detachment, which decreased the protein concentration. However, excessive PL concentrations possibly generated a multilayered membrane structure, with the mixed interface forming a skin-like folded membrane, while the regional presence of multilayered membrane structures increased protein loading (Yesiltas et al., 2019). Research has shown that the involvement of PL resulted in a four-fold higher interfacial protein level than sodium caseinate alone, which was consistent with findings involving globulin (Bylaite et al., 2001).

3.3. Z-potential

Proteins adsorbed in the interfacial layer give bovine milk fat globules a ζ -potential, the value of which reflects the effect of PL on the

composition of MFGM. Fig. 5 presents the ζ -potential values of the different samples. The results showed that the control group displayed the lowest ζ -potential of about -40.47 mV, while 0.15 % PL significantly increased the ζ -potential to -38.27 mV ($p < 0.05$). The proteins on the fat globule surfaces were negatively charged during the continuous phase due to ionization, creating electrostatic repulsion between the fat globules (Xiong et al., 2020). The control group had the highest interfacial protein loading with a corresponding increase in its surface charge density, resulting in a significant decrease in ζ potential. However, the addition of PL leads to a decrease in the concentration of interfacial proteins and the positively charged regions of PL may form complexes with proteins through charge interactions, leading to an increase in ζ -potential. While a lower interfacial protein concentration increased the ζ -potential. As the PL concentration continued to increase, the ζ potential rose slightly but showed no statistical differences ($p > 0.05$). This was possibly because the PL remained in kinetic equilibrium with the proteins after reaching the critical micellar concentration. In addition, high PL concentrations slightly decreased the ζ -potential, possibly due to higher protein loading by the subsequent skin-like folded membranes.

3.4. Interface adsorption behavior

3.4.1. Interfacial tension

The change in interfacial tension caused by protein-PL interactions is closely related to that of emulsion stability, and the interfacial behavior of PL and proteins between water and oil was determined by the pendant drop method. The interfacial tension evolution over time highlighted the PL and protein adsorption process at the O–W interface (Fig. 6A). Protein adsorption at the interface can be divided into three phases:

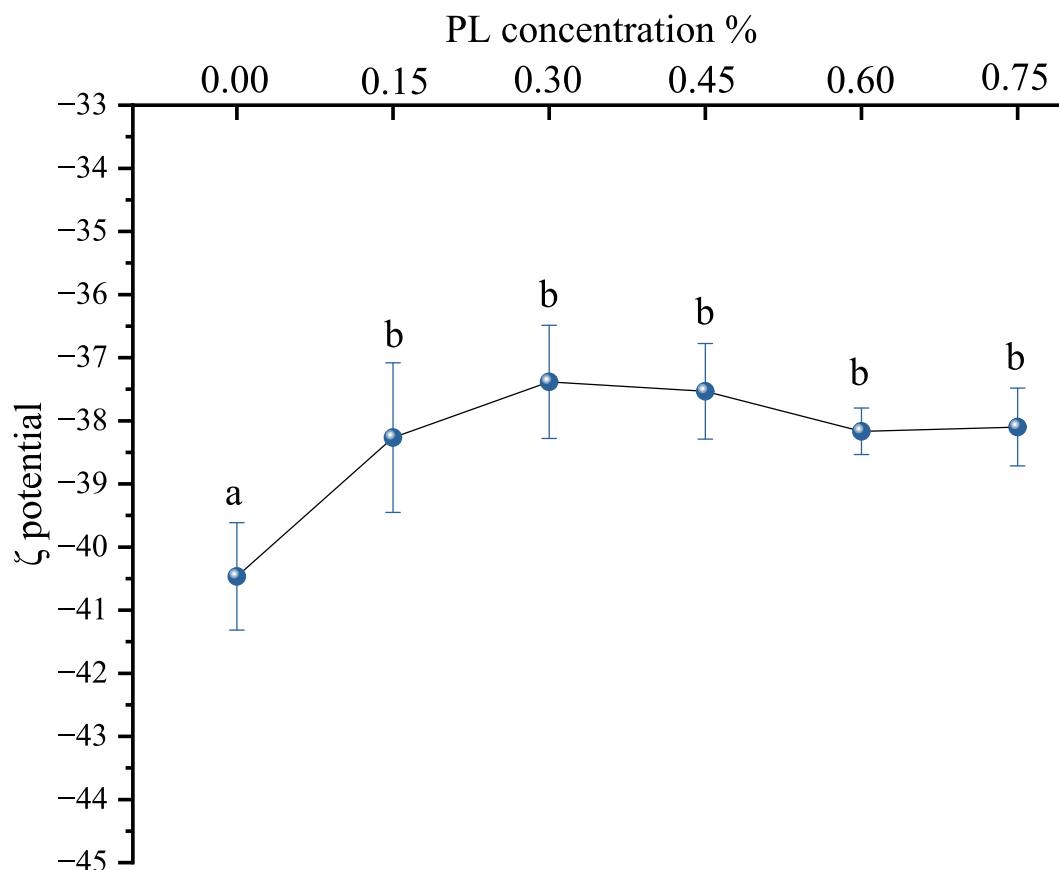


Fig. 5. Effect of different PL concentrations on the ζ -potential of RDC emulsions. Different letters indicate statistically significant differences between samples ($p < 0.05$).

diffusion, permeation/unfolding, and structural rearrangement. The first step in the adsorption process occurs at the instant of droplet formation, when substances in the continuous phase migrate and diffuse toward the O—W interface, a process controlled by a diffusion mechanism that is too short to be measured and is only relevant to the measurement of the instantaneous tension at the beginning of the measurement (Zhou et al., 2021). The blank group without PL was completely stabilized by the proteins at the O—W interface, with an instantaneous interfacial tension of 16.72 mN/m at the beginning of the measurement. In contrast, with the addition of phospholipids, the initial tension decreased significantly, with 0.75 % PL causing a significant reduction in the initial tension to 14.4 mN/m. Subsequently, the PL and proteins that diffuse into the oil-water interface permeate and adsorb at the interfacial layer, and the interfacial layer that is formed leads to a significant reduction in tension. The rate of decrease in interfacial tension is related to the rate of PL and protein adsorption, unfolding and structural rearrangement of proteins, and the interaction between proteins and phospholipids (this will be discussed in detail in 3.4.2). Fig. 6A shows that higher PL concentrations resulted in lower interfacial tension for the same adsorption time, suggesting that the addition of PL increased the efficiency of interfacial layer formation. And the curve tends to flatten at the end point of the test, which is considered that protein unfolding and remodeling are basically completed at this time, and the reconstituted interfacial layer is in a pseudo-equilibrium state. At this time, the interfacial tension of the control group was 15.23 mN/m, while with the increase of PL concentration, the interfacial tension gradually decreased, and the addition of 0.75 % PL reduced the interfacial tension to 9.73 mN/m. This suggests that after droplet formation, competitive adsorption between the emulsifier and the protein was determined leading to the final interfacial morphology. Therefore, and because PL with its smaller molecular structure may fill the gap

between the proteins in the interfacial layer, the interfacial layer PL reduces the tension at the O—W interface with increasing PL concentration. Lower interfacial tension reduced the intermolecular forces and interfacial free energy to promote smaller droplet formation, which was consistent with the droplet size results.

3.4.2. Adsorption kinetics

Furthermore, this study performed adsorption kinetic fitting according to the adsorption behavior shown in Eq. 7 to obtain first-order rate constants of penetration (Kp) and rearrangement (Kr):

$$\ln \frac{\pi_f - \pi_t}{\pi_f - \pi_0} = -kt \quad (7)$$

where π_0 , π_t , and π_f are the interfacial pressures at the beginning, at any time point, and at equilibrium, respectively. Here, k represents the first-order rate constant and t denotes the time.

The protein adsorption kinetics at the O—W interface can be described as a three-step process: diffusion, penetration/unfolding, and rearrangement. The second stage of the surface stabilization process consists of protein penetration (adsorption) at the interface and subsequent protein unfolding, where the interfacial tension decreases dramatically. Fig. 6B shows the kinetic fitting results. The findings indicated a protein Kp of 5.51×10^{-4} 1/s at the interface, while a higher PL addition concentration significantly increased the Kp value. This could be because the smaller molecular weight of PL allowed faster interfacial penetration to reduce the interfacial tension. Therefore, it contributed to MFGM formation. The tension change slowed during the last stage of adsorption, gradually reaching an equilibrium state corresponding to the second linear region showed in Fig. 6B. In the absence of PL, the Kr of protein was 3.43×10^{-3} 1/s, which was increased significantly by PL addition, reaching a maximum of 8.36×10^{-3} 1/s at 0.75

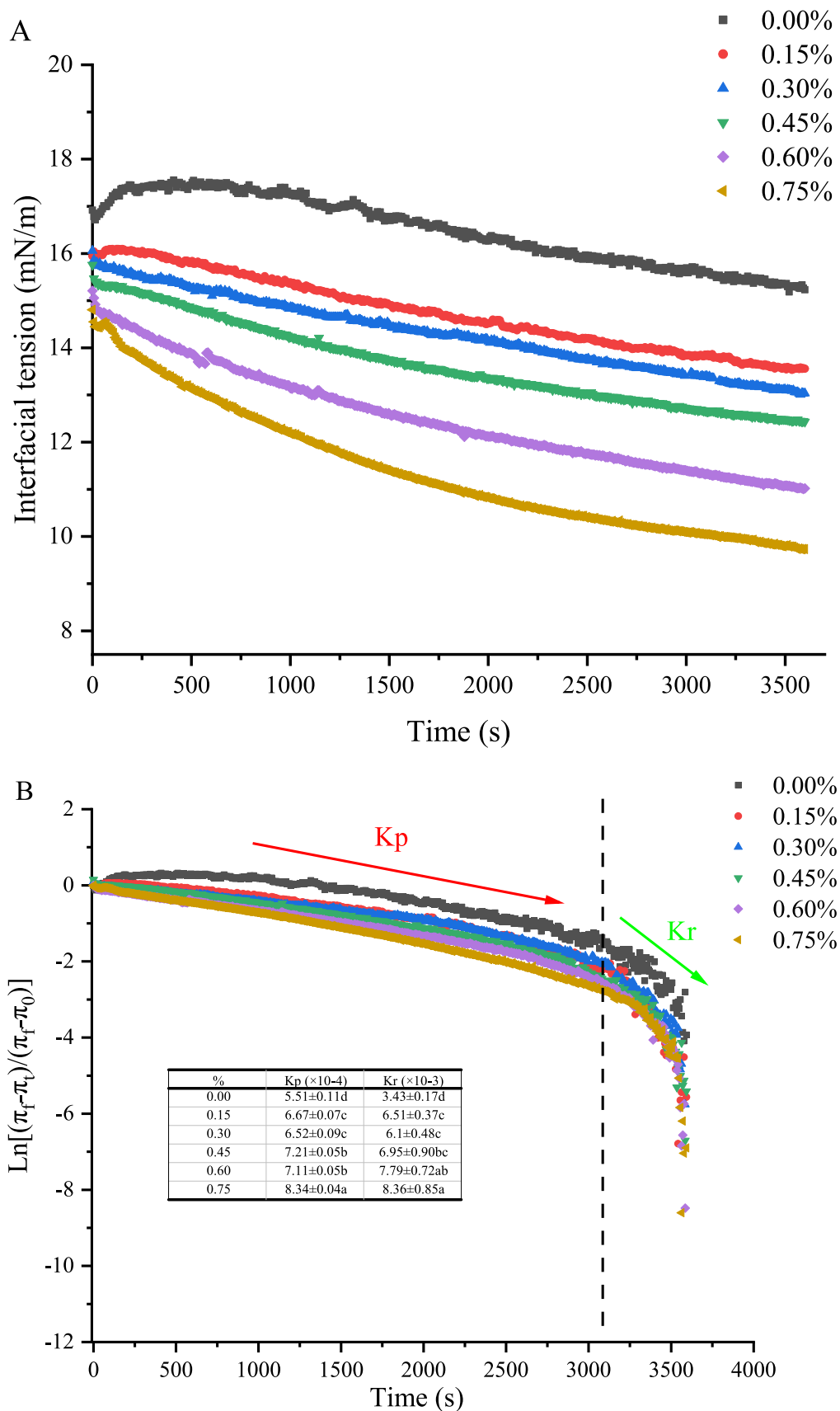


Fig. 6. Effects of different PL concentrations on time-tension curves (A), adsorption kinetics (B) and interfacial rheology (D) at the oil-water interface. Schematic representation of the relationship between different PL concentrations and proteins at the interface (C). Different letters indicate statistically significant differences between samples ($p < 0.05$).

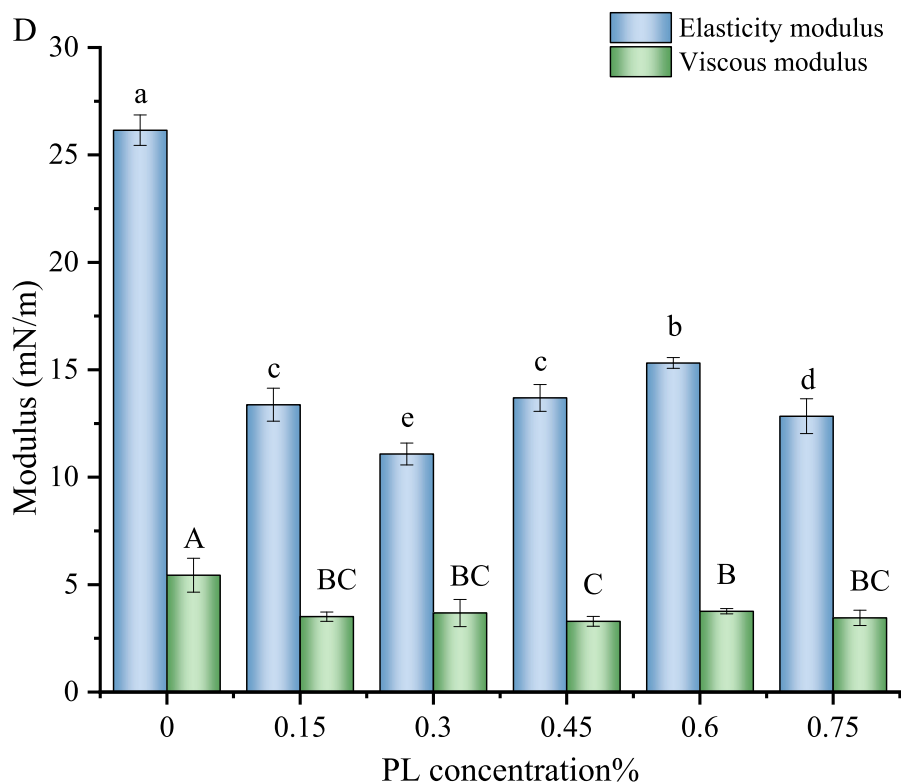
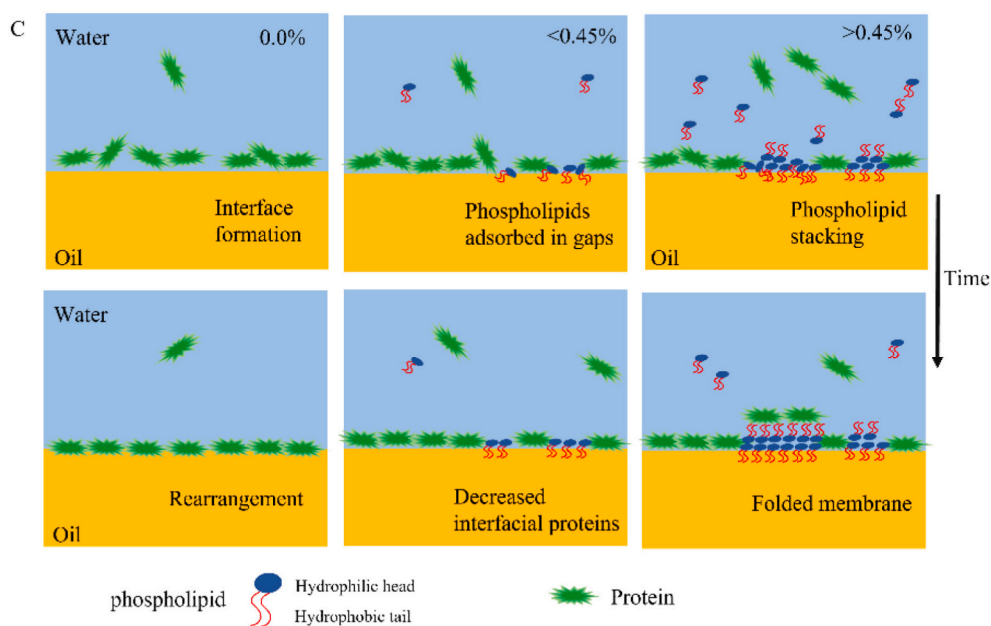


Fig. 6. (continued).

%. During this stage, the adsorbed proteins continued to reorient themselves toward an energetically more favorable conformation. The higher K_r value indicated that the addition of PL intensified interfacial layer rearrangement.

A model emphasizing the relationship between PL and proteins was used to explain the MFGM properties at different concentrations. The PL and protein permeation and rearrangement at the O–W interface are depicted separately in Fig. 6C. During interfacial formation, proteins penetrate the interface and adsorb rapidly, providing initial stability. As the interfacial layer improves, adsorption rate shows a gradual decline, causing the haphazardly stacked proteins to rearrange and reduce the

protein layer energy. The addition of PL changed this state. The smaller size of PL allowed adsorption in the gaps between the protein links, more efficiently reducing the interfacial layer tension. Therefore, PL addition gradually decreased the interfacial tension. In addition, PL adsorption and compaction may cause protein desorption via orogenic displacement, which decreases the interfacial protein content and significantly increases the K_r (Zhang, Fan, et al., 2022). Higher PL accumulation at the interface can exacerbate rearrangement and may cause skin-like folding of the interfacial layer due to multilayer protein adsorption, possibly causing fat globule attachment.

3.4.3. Interfacial rheology

The rheological properties of the interfacial layer at pseudo-equilibrium was analyzed via interfacial dilatational rheology to reflect the state of the interfacial layer in dynamic environments and clarify the impact of emulsifiers on protein adsorption and molecular interactions (Zhang, Diao, et al., 2022). The dynamic stability of the reconstituted fat globule interfacial layer is generally related to E' and E'' at the O–W interface. Fig. 6D shows the rheological properties of the different RDC emulsions. The interfacial layers of the different fat globules generally displayed $E'' < E'$, indicating that the droplet surfaces exhibited elastic behavior during oscillatory expansion. This could maintain the spatial independence of the droplets. The protein-stabilized interfacial layer displayed the largest E' of 26.15 mN/m, indicating that the interfacial layer exhibited higher mechanical strength. PL addition significantly reduced the E' of the interfacial layer, with the lowest E' of 11.08 mN/m at 0.3%. On the one hand, this may be because competitive PL and protein adsorption reduces the interfacial protein concentration. On the other hand, insufficient protein adsorption at the O–W interface allows PL to fill the gaps between the proteins. Therefore, the proteins are only loosely bound in an irregular pattern. Zhang, et al. (Zhang et al., 2022) concluded that emulsifiers displayed weaker interactions at the O–W interface and were less resistant to deformation. Similar to the interfacial protein concentration, the E' increased significantly as the PL concentration continued to rise. This is closely related to the increase in the interfacial protein content due to a high PL concentration.

3.5. Thermodynamic properties

RDC requires complete aging at 4 °C before aeration. The thermodynamic properties of milk fat crystallization during this process are crucial for the physicochemical properties of whipped cream (Du et al., 2021). The effect of emulsifiers may contribute to fat crystallization by promoting or inhibiting fat nucleation, crystal growth, polycrystalline transition, and crystal interaction (Zeng et al., 2021). The DSC data provided a reference for fat crystallization in the RDC emulsion, as shown in Fig. 7. No phase transition occurred during sample cooling

from 45 °C to 15 °C. Furthermore, no changes were evident in the heat flow, indicating that the starting crystallization temperatures of the milk fats were all below 15 °C. The control without added PL presented an onset crystallization temperature of 15.04 °C, a primary crystallization temperature of 12.14 °C, and the presence of a shoulder peak at 5–6 °C. PL addition decreased the initial crystallization temperature of the samples. The results showed that 0.15% PL decreased the initial crystallization temperature to 13.48 °C, which declined even further to 10.56 °C at a 45% PL concentration. The main crystallization temperature was 8.33 °C, while the shoulder peak basically disappeared. Some types of emulsifiers are used as seeds for crystallization, accelerating the nucleation rate before the triglyceride crystallizes, or crystallizing with the triglyceride and acting as crystal structure modifiers (Zeng et al., 2021). Conversely, PL addition decreased the fat crystallization temperature, possibly delaying nucleation by disrupting the primary fat molecule organization (Delacharlerie et al., 2016). Furthermore, no changes were evident in the initial and main crystallization temperatures at PL concentrations higher than 0.45%, indicating that the crystallization behavior was no longer affected by the PL concentration. This may be due to the limited solubility of PL in AMF, where excess PL may remain in the continuous phase and be difficult to act due to the presence of polar heads (Vanhoutte et al., 2002).

3.6. Crystallization kinetics

Isothermal crystallization kinetics can provide vital insight into crystallization behavior (Zhang et al., 2019). The Avrami model was used to fit the fat crystallization zone, as shown in Table 1. The Avrami exponent (n) reflects the crystal growth pattern. Its value is theoretically an integer, referring to the sum of the spatial dimension of the growth and the temporal dimension of the nucleation process. Higher n values indicate higher nucleation growth dimensions or a shift in the nucleation mechanism from transient to sporadic nucleation (Cheng et al., 2020). The control group displayed the highest n of 2.03, indicating sporadic nucleation and discoidal growth in the fat, possibly leading to uneven crystal formation. This was consistent with the PLM analysis (Fig. 8). PL addition decreased the Avrami exponent to between 1.52

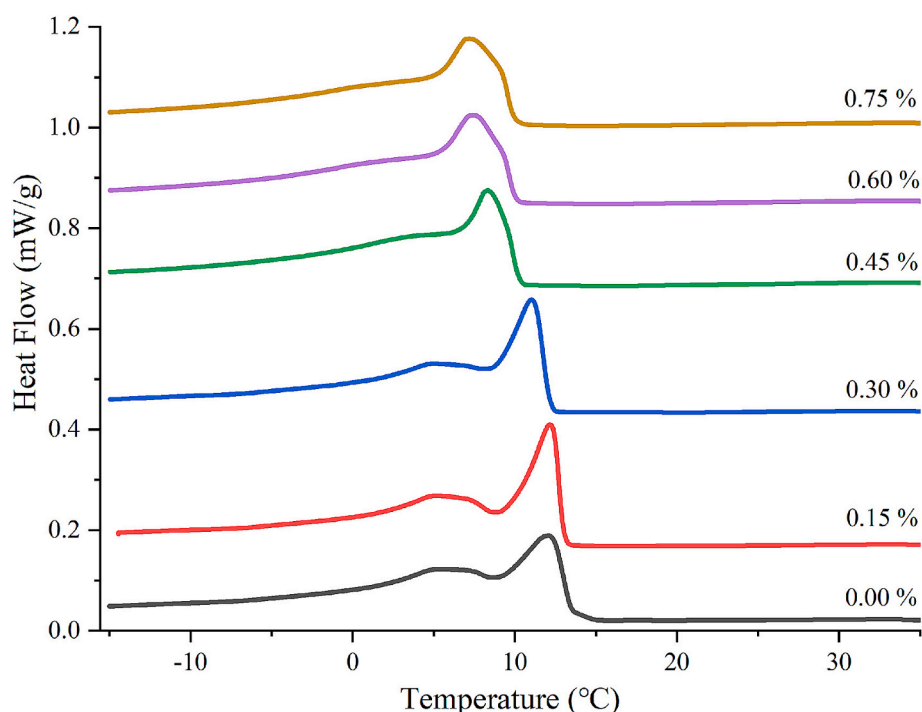


Fig. 7. Effect of different PL concentrations on the thermodynamic properties of RDC emulsions.

Table 1

The Avrami exponent (n) and crystallization rate constant (K) of RDC emulsions with different lecithin concentrations.

Lecithin concentration (%)	Avrami exponent(n)	Crystallization rate constants (K)	R ²
0.00%	2.03 ± 0.01 ^a	0.48 ± 0.002 ^a	0.97
0.15 %	1.55 ± 0.01 ^d	0.66 ± 0.003 ^c	0.95
0.30 %	1.52 ± 0.01 ^e	0.71 ± 0.003 ^e	0.97
0.45 %	1.67 ± 0.01 ^b	0.68 ± 0.003 ^d	0.97
0.60 %	1.67 ± 0.01 ^b	0.57 ± 0.002 ^b	0.97
0.75 %	1.63 ± 0.01 ^c	0.58 ± 0.002 ^b	0.98

Different letters in the same column indicate statistically significant differences between samples ($p < 0.05$).

and 1.67, while the crystallization behavior showed transient nucleation and more significant crystal formation. This may be because PL act as non-homogeneous nucleation sites to induce crystalline nucleation (Svanberg et al., 2011). In addition, Matsumiya et al. (2017) reported that droplet size changes also affected supercooled nucleation and partial coalescence. The crystallization rate constant k is related to the nucleation and crystal growth rates. The control group displayed a crystallization rate constant k of 0.48, which increased significantly to 0.71 when the PL concentration increased from 0.00 % to 0.30 % ($p < 0.05$). This may be because PL increases transient nucleation and the number of nucleation sites. Higher k values and lower n values generally indicate smaller crystals during crystallization (Zhang et al., 2019). A 0.75 % PL concentration significantly decreased the k value to 0.58 ($p < 0.05$), suggesting that high PL concentrations slowed the fat crystallization rate, which may be due to the crystalline linkages induced by excess PL. Similarly, Delacharlerie et al. (2016) suggested that PL altered crystal morphology by blocking specific surfaces, consequently slowing

recrystallization and polycrystalline transformation. As shown in Fig. 7, the crystallization onset temperature of the emulsion showed a decreasing trend with the increase of PL concentration, which indicates that there is an intrinsic correlation between the change of crystallization temperature in the system and the regulation of the crystallization rate.

3.7. Whipping characteristics of the RDC

3.7.1. Whipping time

RDC aeration is a complex process, which is influenced by various factors such as fat crystallization, interfacial strength, and rheological properties. The process consists of three phases: rapid inflation, bubble encapsulation, and stabilization. Fat globule-mediated partial coalescence and protein adsorption are believed to be the key factors in inflation (Yan et al., 2022). Fig. 9A shows the effect of different PL concentrations on the RDC whipping characteristics. Compared with the control group, 0.15 % PL significantly decreased the aeration time from 12.45 min to 3.67 min, while the churning time was further reduced as the PL concentration increased. However, no significant decrease was evident the RDC whipping time at PL concentrations exceeding 0.3 %. Inflation is primarily affected by the partial coalescence rate of the fat globules during mixing and the formation of a stable lipid network. The fat globule interface of the blank fraction was covered with a complete protein layer and exhibited a higher interfacial strength, which prevented crystal bridging between fat globules and consequently required a longer mixing time for stable inflatable structure formation (Yan et al., 2024). PL affected the composition of the interfacial layer and reduced the interfacial protein content, which decreased the interfacial layer strength. Therefore, the fat globules were more susceptible to partial coalescence, which reduced the churning time.

3.7.2. Overrun

Fig. 9B shows the whipped cream expansion. The control group

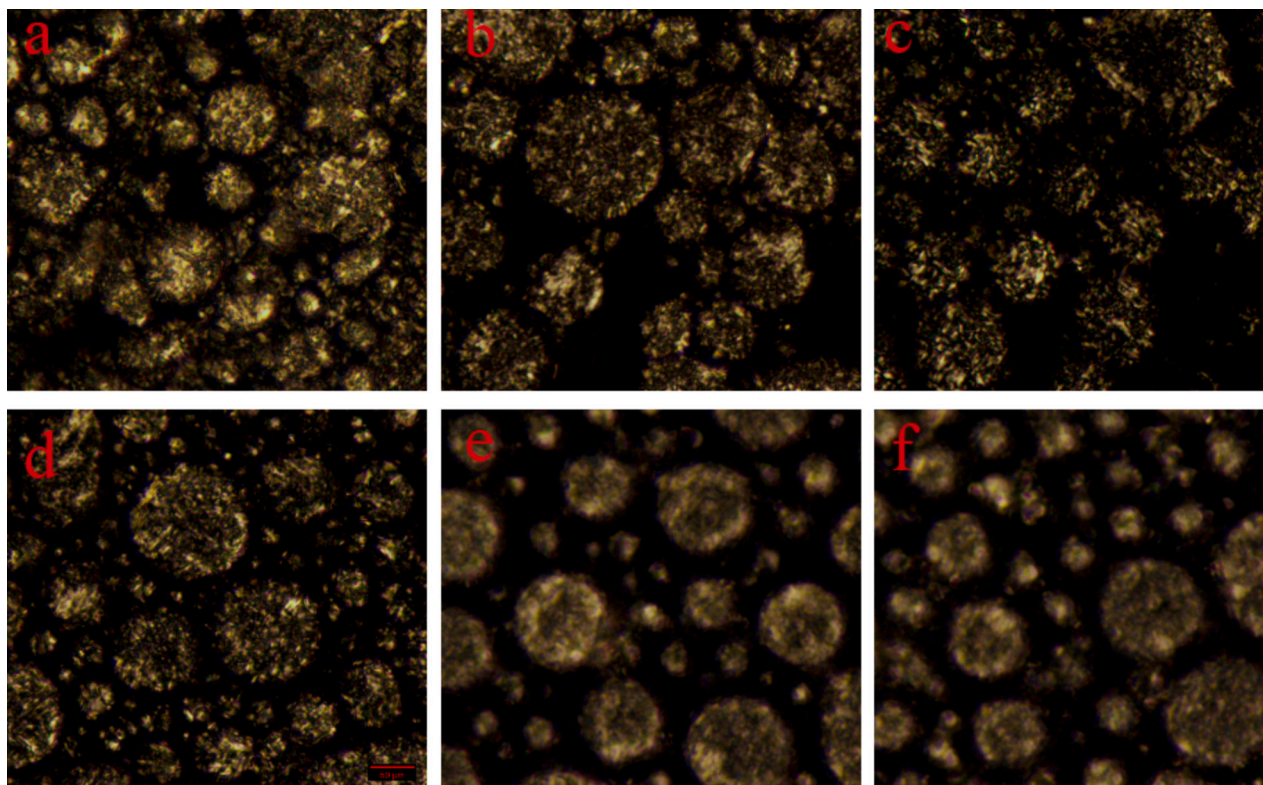


Fig. 8. Polarized light microscopic images of RDC emulsions with different PL concentrations. Where a-f represents lecithin concentration 0.00 % - 0.75 %.

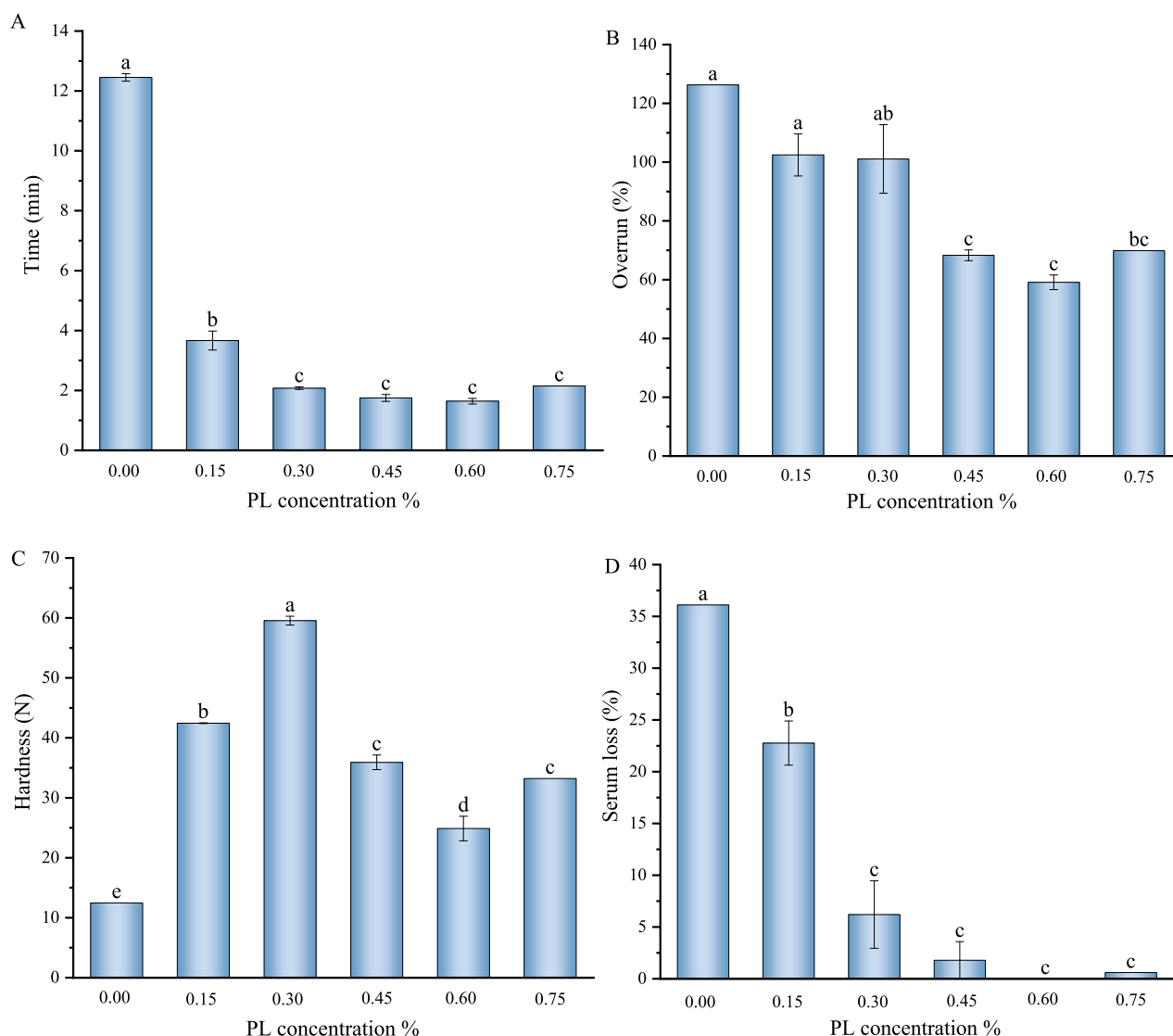


Fig. 9. Effect of different PL concentrations on RDC whipping time (A), overrun (B), hardness (C) and serum loss (D). Different letters indicate statistically significant differences between samples ($p < 0.05$).

displayed the highest overrun of 126.32 %, which was reduced to 102.48 % and 101.08 %, respectively, by 0.15 % and 0.30 % PL, with no significant differences ($p > 0.05$). The whipped cream overrun decreased even further as the PL continued to increase PL ($p < 0.05$). Whipped cream is a solid foam structure that essentially transforms from an O–W RDC emulsion system to a foam system stabilized by proteins and fat globules (Salonen, 2020), as shown by the microstructure in Fig. 10. During the first stage of whipping, the air was quickly encapsulated by the continuous phase proteins to form bubbles. The fat globules bound the bubbles by generating a network structure via crystal bridging to form a stable foam structure (Blankart et al., 2023). PL addition significantly increased the fat globule coalescence rate and reduced the RDC whipping time, which decreased the number of bubbles in the continuous-phase protein packages and subsequent expansion. Contrarily, the increased viscosity at high concentrations limited air encapsulation, further reducing the overrun.

3.7.3. Texture

The textural properties of the whipped cream were analyzed to evaluate the effect of PL on the foam quality, as shown in Fig. 9C. The whipped cream without added PL exhibited the lowest hardness of about 12.48 N, while PL addition significantly increased the hardness, with

0.3 % PL yielding the highest value of 59.55 N. PL addition reduced the whipped cream overrun, which increased the viscosity, structural strength, and stability of the foam. Contrarily, the hardness of the whipped cream decreased as the PL concentration continued to increase ($p < 0.05$), which could be because the higher interfacial protein content reduced the crystal bridging of the droplets. As shown in the microstructure of Fig. 10, the degree of agglomeration of fat globules in RDC increased significantly with increasing PL concentration, which contributed to the attachment and stabilization of the foam structure, and the whipped cream had a higher hardness. On the contrary, with the increase of PL, the bubble size in the cream gradually increased and concentrated (Figure 10A1-D1), and the bubble size in the 0.6 % PL sample was about 122 μm , for which was not conducive to the expansion and stabilization of the foam structure, and thus the high concentration of PL led to a decrease in the hardness of the whipped cream. It is noteworthy that the bubbles formed in the sample containing 0.15 % PL were encapsulated by green-labeled proteins (Figure 10A2), whereas the protein layer gradually appeared to be nicked as PL increased, and Figure 10D3 shows the absence of the protein layer on the surface of the bubbles, which suggests that PL is involved in the formation and stabilization of the bubbles.

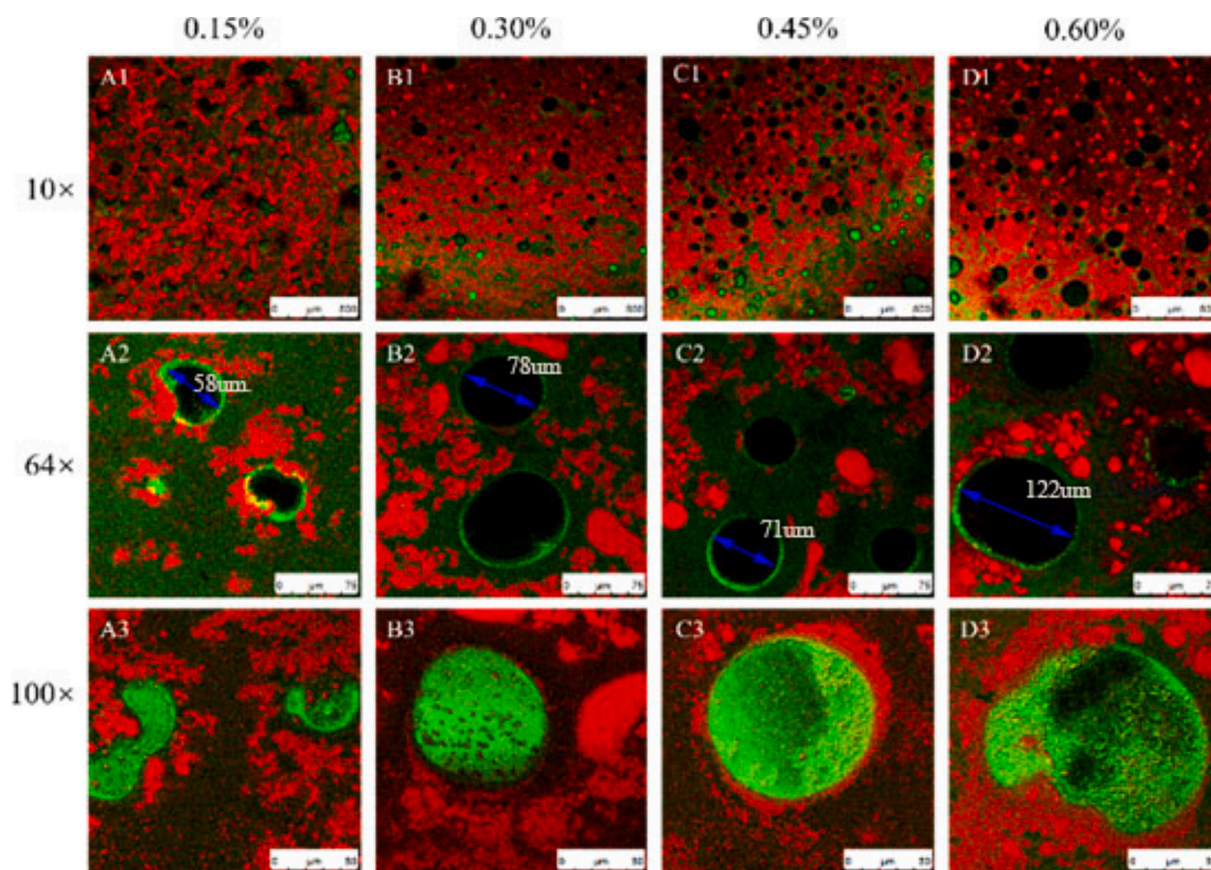


Fig. 10. Effect of different PL concentrations on the microstructure of whipped cream. The red signals in the image represent fat, the green signals represent protein, and the black circular areas represent the interior of bubbles. (For interpretation of the references to colour in this figure legend, the reader is referred to the web version of this article.)

3.7.4. Foam stability

Foam system stability is vital for whipped cream quality and can be expressed in terms of serum loss (Fig. 9D). The serum loss in the control sample without PL was about 36.10 %, which declined significantly to 22.8 % after adding 0.15 % PL, while the 0.3 % fraction was further reduced to 1.79 % ($p < 0.05$). Drainage and aggregation are the primary factors that can cause bubble destabilization. PL addition increased the system viscosity, which limited bubble movement and the aqueous phase (Dutta et al., 2004), reducing serum loss. In addition, analysis of the whipped cream microstructure indicated that a higher PL concentration increased fat globule adsorption on the foam surface. This may be related to fat globule aggregation due to higher PL levels, which increased the connection between the fat globules.

4. Conclusions

The results of this study emphasize the potential of PL in improving RDC emulsion stability and enhancing whipped cream quality, which is closely related to the PL concentration. Increasing the PL concentration in a range of 0–0.45 % significantly decreases the O–W interfacial tension and the size of the recombined droplets, while the emulsion viscosity and stability rise substantially. In addition, PL and protein adsorption competition during fat globule membrane reconstitution decreases interfacial protein loading and layer strength, which significantly reduces the RDC churning time and overrun, while increasing the whipped cream hardness. Contrarily, the possible PL multilayer adsorption on the fat globule membrane at high concentrations (>0.45 %) leads to skin-like membrane folding, which increases the interfacial protein concentration and fat globule size. The interaction between the fat globules further increases the emulsion viscosity, which enhances the

emulsion and whipped cream stability. In addition, although incorporating PL as a non-homogeneous nucleating agent increases microcrystal formation and the number of nucleation sites in the droplets, it significantly reduces the initial fat crystallization temperature. These findings are useful for improving the quality of whipped dairy products.

However, we have also only studied the initial state of the PL-reorganized interfacial layer and have not conducted a long-term study. Since emulsions tend to have a long shelf life and proteins may be replaced by emulsifiers over time, the long-term stability between the interfacial layer and the emulsion needs to be further investigated. In addition, some low molecular emulsifiers and polysaccharides, also affect the physicochemical properties in whipped cream systems, and attention must be paid to the interaction mechanisms of these components.

CRediT authorship contribution statement

Guosen Yan: Writing – review & editing, Writing – original draft, Visualization, Software, Methodology, Investigation, Data curation. **Pan Zhao:** Software, Methodology, Investigation. **Zhenbo Shao:** Software, Formal analysis. **Yiting Li:** Software, Formal analysis. **Jie Han:** Methodology, Investigation, Data curation. **Yan Li:** Resources, Methodology, Funding acquisition, Conceptualization. **Liebing Zhang:** Resources, Funding acquisition.

Declaration of competing interest

The authors declare that they have no known competing financial interests or personal relationships that could have appeared to influence the work reported in this paper.

Acknowledgment

This research was supported by the earmarked fund for CARS 36 and the Key R & D program of the Ningxia Hui Autonomous Region (No. 2024BEE02022).

Appendix A. Supplementary data

Supplementary data to this article can be found online at <https://doi.org/10.1016/j.fochx.2025.102547>.

Data availability

Data will be made available on request.

References

- Atik, D. S., Bölük, E., Toker, O. S., Palabiyik, I., & Konar, N. (2020). Investigating the effects of lecithin-PGPR mixture on physical properties of milk chocolate. *Lwt*, *129*, Article 109548.
- Bernaschina, M., Leser, M. E., Limbach, H. J., Fischer, P., & Roucher, A. (2024). Lentil protein stabilized emulsion-impact of lecithin addition on emulsions properties. *Food Hydrocolloids*, *147*, Article 109337.
- Blankart, M., Hetzer, B., & Hinrichs, J. (2023). Similar but not equal—a study on the foam stabilisation mechanism of mechanically whipped cream and aerosol whipping cream. *International Dairy Journal*, *139*, Article 105562.
- Bylaite, E., Nylander, T., Venskutonis, R., & Jönsson, B. (2001). Emulsification of caraway essential oil in water by lecithin and β -lactoglobulin: Emulsion stability and properties of the formed oil–aqueous interface. *Colloids and Surfaces B: Biointerfaces*, *20*(4), 327–340.
- Cheng, J., Dudu, O. E., Li, X., & Yan, T. (2020). Effect of emulsifier-fat interactions and interfacial competitive adsorption of emulsifiers with proteins on fat crystallization and stability of whipped-frozen emulsions. *Food Hydrocolloids*, *101*, Article 105491.
- Cheng, J., Kan, Q., Cao, J., Dudu, O. E., & Yan, T. (2021). Interfacial compositions of fat globules modulate coconut oil crystallization behavior and stability of whipped-frozen emulsions. *Food Hydrocolloids*, *114*, Article 106580.
- Cooper, Z., Simons, C., & Martini, S. (2019). Retardation of crystallization through the addition of dairy phospholipids. *Journal of the American Oil Chemists' Society*, *96*(11), 1205–1218.
- Delacharlerie, S., Petrut, R., Deckers, S., Flöter, E., Blecker, C., & Danthine, S. (2016). Structuring effects of lecithins on model fat systems: A comparison between native and hydrolyzed forms. *LWT - Food Science and Technology*, *72*, 552–558.
- Dhungana, P., Truong, T., Bansal, N., & Bhandari, B. (2019). Apparent thermal and UHT stability of native, homogenized and recombined creams with different average fat globule sizes. *Food Research International*, *123*, 153–165.
- Du, L., Jiang, Q., Li, S., Zhou, Q., Tan, Y., & Meng, Z. (2021). Microstructure evolution and partial coalescence in the whipping process of oleofoams stabilized by monoglycerides. *Food Hydrocolloids*, *112*, Article 106245.
- Dutta, A., Chengara, A., Nikolov, A. D., Wasan, D. T., Chen, K., & Campbell, B. (2004). Destabilization of aerated food products: Effects of Ostwald ripening and gas diffusion. *Journal of Food Engineering*, *62*(2), 177–184.
- Fredrick, E., Heyman, B., Moens, K., Fischer, S., Verwijlen, T., Moldenaers, P., Van der Meeren, P., & Dewettinck, K. (2013). Monoacylglycerols in dairy recombined cream: II. The effect on partial coalescence and whipping properties. *Food Research International*, *51*(2), 936–945.
- Goibier, L., Pillement, C., Monteil, J., Faure, C., & Leal-Calderon, F. (2019). Emulsification of non-aqueous foams stabilized by fat crystals: Towards novel air-in-oil-in-water food colloids. *Food Chemistry*, *293*, 49–56.
- Gutiérrez Méndez, N., Chavez Garay, D. R., & Leal Ramos, M. Y. (2022). Lecithins: A comprehensive review of their properties and their use in formulating microemulsions. *Journal of Food Biochemistry*, *46*(7), Article e14157.
- Ihara, K., Hirota, M., Akitsu, T., Urakawa, K., Abe, T., Sumi, M., Okawa, T., & Fujii, T. (2015). Effects of emulsifying components in the continuous phase of cream on the stability of fat globules and the physical properties of whipped cream. *Journal of Dairy Science*, *98*(5), 2875–2883.
- Koocheki, A., Kadkhodae, R., Mortazavi, S. A., Shahidi, F., & Taherian, A. R. (2009). Influence of Alyssum homolocarpum seed gum on the stability and flow properties of O/W emulsion prepared by high intensity ultrasound. *Food Hydrocolloids*, *23*(8), 2416–2424.
- Li, Y., Li, Y., Yan, G., Wang, S., Wang, Y., Li, Y., Shao, Z., Wang, H., & Zhang, L. (2024). Dry fractionation efficiency of milk fats from different sources and the characteristics of their fractions in chemical composition, thermal property, and crystal morphology. *Food Chemistry: X*, *22*, Article 101350.
- Liu, Z., Cao, Z., Zhao, M., Zhang, H., Wang, J., & Sun, B. (2022). Synergistic influence of protein particles and low-molecular-weight emulsifiers on the stability of a milk fat-based whippable oil-in-water emulsion. *Food Hydrocolloids*, *127*, Article 107520.
- Lu, N., Wang, J., Chen, Z., Zhang, X., Chen, C., & Wang, S. (2021). The effect of adding phospholipids before homogenization on the properties of milk fat globules. *Lwt*, *146*, Article 111659.
- Matsumiya, K., Horiguchi, S., Kosugi, T., Mutoh, T., Nambu, Y., Nishimura, K., & Matsumura, Y. (2017). Effects of heat treatment and homogenization on milk fat globules and proteins in whipping creams. *Food Structure*, *12*, 94–102.
- Pal, R. (1998). A novel method to correlate emulsion viscosity data. *Colloids and Surfaces A: Physicochemical and Engineering Aspects*, *137*(1–3), 275–286.
- Patel, A. R., & Dewettinck, K. (2015). Current update on the influence of minor lipid components, shear and presence of interfaces on fat crystallization. *Current Opinion in Food Science*, *3*, 65–70.
- Salonen, A. (2020). Mixing bubbles and drops to make foamed emulsions. *Current Opinion in Colloid & Interface Science*, *50*, Article 101381.
- Svanberg, L., Ahrné, L., Lorén, N., & Windhab, E. (2011). Effect of sugar, cocoa particles and lecithin on cocoa butter crystallisation in seeded and non-seeded chocolate model systems. *Journal of Food Engineering*, *104*(1), 70–80.
- Thum, C., Roy, N. C., Everett, D. W., & McNabb, W. C. (2023). Variation in milk fat globule size and composition: A source of bioactives for human health. *Critical Reviews in Food Science and Nutrition*, *63*(1), 87–113.
- Vanhoutte, B., Dewettinck, K., Foubert, I., Vanlerberghe, B., & Huyghebaert, A. (2002). The effect of phospholipids and water on the isothermal crystallisation of milk fat. *European Journal of Lipid Science and Technology*, *104*(8), 490–495.
- Wang, Y., Yuan, D., Li, Y., Li, M., Wang, Y., Li, Y., & Zhang, L. (2019). Thermodynamic and whipping properties of milk fat in whipped cream: A study based on DSC and TD-NMR. *International Dairy Journal*, *97*, 149–157.
- Xiong, X., Ho, M. T., Bhandari, B., & Bansal, N. (2020). Foaming properties of milk protein dispersions at different protein content and casein to whey protein ratios. *International Dairy Journal*, *109*, Article 104758.
- Xu, H., Gao, Z., Huang, M., Fan, Q., Cui, L., Xie, P., Liu, L., Guan, X., Jin, J., & Jin, Q. (2024). Static stability of partially crystalline emulsions stabilized by milk proteins: Effects of κ -carrageenan, λ -carrageenan, ι -carrageenan, and their blends. *Food Hydrocolloids*, *147*, Article 109387.
- Yan, G., Li, Y., Wang, H., Cui, S., Li, Y., Zhang, L., & Yan, J. (2024). Multiscale approach to the characterization of the interfacial properties of micellar casein and whey protein blends and their effects on recombined dairy creams. *Food Research International*, *114453*.
- Yan, G., Wang, S., Li, Y., Zhang, J., Ding, H., Li, Y., & Zhang, L. (2022). Effect of different polymerization degrees and fatty acids of polyglycerol esters on the physical properties and whippability of recombined dairy cream. *Foods*, *12*(1), 22.
- Yan, J., Yang, Z., Qiao, X., Kong, Z., Dai, L., Wu, J., ... McClements, D. J. (2022). Interfacial characteristics and in vitro digestion of emulsion coated by single or mixed natural emulsifiers: Lecithin and/or rice glutelin hydrolysates. *Journal of the Science of Food and Agriculture*, *102*(7), 2990–2999.
- Yesiltas, B., Torkkeli, M., Almásy, L., Dudás, Z., Wacha, A. F., Dalgiesh, R., ... Knaapila, M. (2019). Interfacial structure of 70% fish oil-in-water emulsions stabilized with combinations of sodium caseinate and phosphatidylcholine. *Journal of Colloid and Interface Science*, *554*, 183–190.
- Zeng, D., Cai, Y., Liu, T., Huang, L., Liu, P., Zhao, M., & Zhao, Q. (2021). Effect of sucrose ester S370 on interfacial layers and fat crystals network of whipped cream. *Food Hydrocolloids*, *113*, Article 106541.
- Zeng, Y., Zeng, D., Liu, T., Cai, Y., Li, Y., Zhao, M., & Zhao, Q. (2022). Effects of glucose and corn syrup on the physical characteristics and whipping properties of vegetable-fat based whipped creams. *Foods*, *11*(9), 1195.
- Zhang, M., Fan, L., Liu, Y., Huang, S., & Li, J. (2022). Effects of proteins on emulsion stability: The role of proteins at the oil–water interface. *Food Chemistry*, *397*, Article 133726.
- Zhang, Y., Diao, Y., Zhang, W., Xu, W., Hu, Z., & Yi, Y. (2022). Influence of molecular structure and interface behavior on foam properties of rice bran protein nanoparticles. *Lwt*, *163*, Article 113537.
- Zhang, Z., Lee, W. J., Zhou, H., & Wang, Y. (2019). Effects of chemical interesterification on the triacylglycerols, solid fat contents and crystallization kinetics of palm oil-based fats. *Food & Function*, *10*(11), 7553–7564.
- Zhou, B., Tobin, J. T., Drusch, S., & Hogan, S. A. (2021). Interfacial properties of milk proteins: A review. *Advances in Colloid and Interface Science*, *295*, 102347.
- Zhou, X., Chen, L., Han, J., Shi, M., Wang, Y., Zhang, L., Li, Y., & Wu, W. (2016). Stability and physical properties of recombined dairy cream: Effects of soybean lecithin. *International Journal of Food Properties*, *20*.